Protocol

Long-Term, High-Resolution Imaging in the Neocortex In Vivo

Brian E. Chen, Joshua T. Trachtenberg, Anthony J.G.D. Holtmaat, and Karel Svoboda

This protocol was adapted from "Long-Term, High-Resolution Imaging in the Neocortex In Vivo," Chapter 23, in *Live Cell Imaging* (eds. Goldman and Spector). Cold Spring Harbor Laboratory Press, Cold Spring Harbor, NY, USA, 2005.

INTRODUCTION

In the neocortex, elucidating the mechanisms of structural plasticity is essential to an understanding of the emergent network properties and fundamental cognitive phenomena, such as memory formation. Time-lapse imaging microscopy has revealed a remarkable array of dynamic activities in dendritic structures in developing cortical tissue in vitro, the developing cortex in vivo, and even the adult neocortex. Chronic high-resolution in vivo imaging of the structure of neurons in the cortex became possible with the invention of two-photon laser scanning microscopy (2PLSM). This technique has key advantages over conventional, single-photon excitation techniques, such as confocal microscopy. Two-photon excitation is the near-simultaneous (within femtoseconds) absorption of two photons coinciding on a fluorophore. The absorption rate depends quadratically on the illumination intensity and is therefore confined to a small volume around the focal point. Scattered excitation light is too weak to generate fluorescence. Thus, the signal is generated exclusively in a tiny focal volume, and all emitted fluorescence photons constitute useful signals. A related advantage is that the longer wavelengths used to generate two-photon excitation penetrate scattering tissue more efficiently than the shorter wavelengths used to generate single-photon excitation of the same fluorophores. The upper layers (1-4) of neocortex are ideal for high-resolution 2PLSM imaging. This protocol describes experimental procedures for in vivo imaging in the neocortex.

RELATED INFORMATION

Scattering length increases approximately linearly with increasing wavelengths (Oheim et al. 2001). In the cortex, the scattering length at 800-nm wavelength, $l_s^{(800)}$, measured in vivo is ~100 µm (Kleinfeld et al. 1998) and appears to decrease with increasing age (Oheim et al. 2001). Typically, imaging is limited to the most superficial 500 µm of the tissue.

MATERIALS

CAUTIONS AND RECIPES: Please see Appendices for appropriate handling of materials marked with <**!**>, and recipes for reagents marked with <**R**>.

Reagents

Acrylic, dental
<**R**>Agarose (1.5%) for neocortex imaging
<**!**>Cyanoacrylate

<!>Dexamethasone (4 mg/mL)
Gelfoam (Pharmacia/Pfizer) or Avitene Ultrafoam (Davol)

Prior to use, cut the foam into ~7-mm^2 blocks and soak in sterile cortex buffer.

<R><!>Sterile cortex buffer
<R><!>Urethane (20%) (optional; see Step 1).

Urethane can only be used for nonrecovery studies. Humane treatment of animals must be observed at all times and should follow the institutional care and use guidelines for animals.

<R><!>Xylazine/ketamine for imaging (optional; see Step 1)

Equipment

Bar, titanium (with tapped screw holes)
Coverglass (No. 1 thickness)

Custom-make a circular coverglass with a 7-mm diameter.

Drill, dental (with 1/4 bit)
Imaging equipment

*In all experiments involving in vivo imaging of green fluorescent protein/ yellow fluorescent protein (GFP/YFP) expressing neurons in the cortex, we use a custom-built 2PLSM, which is basically a laser-scanning microscope (*Fig. 1*) (Pawley 1995). The light source is typically a mode-locked Titanium:Sapphire laser (Tsunami, Spectra-Physics) running at λ ~910 nm (producing excitation light with wavelengths in the range of 780-980 nm), pumped by a 10-W solid-state laser (Millenia X, Spectra-Physics). The objective (40X, 0.8 NA) and scan lens are from Zeiss, the trinoc from Olympus, and the photomultiplier tube from Hamamatsu. Fluorescence is collected in an epifluorescence mode and the image is constructed in a computer (*Fig. 1*) (Denk et al. 1990). Images are acquired with custom software (MatLab).*

Syringe, sharp
Tools, surgical (sterile)

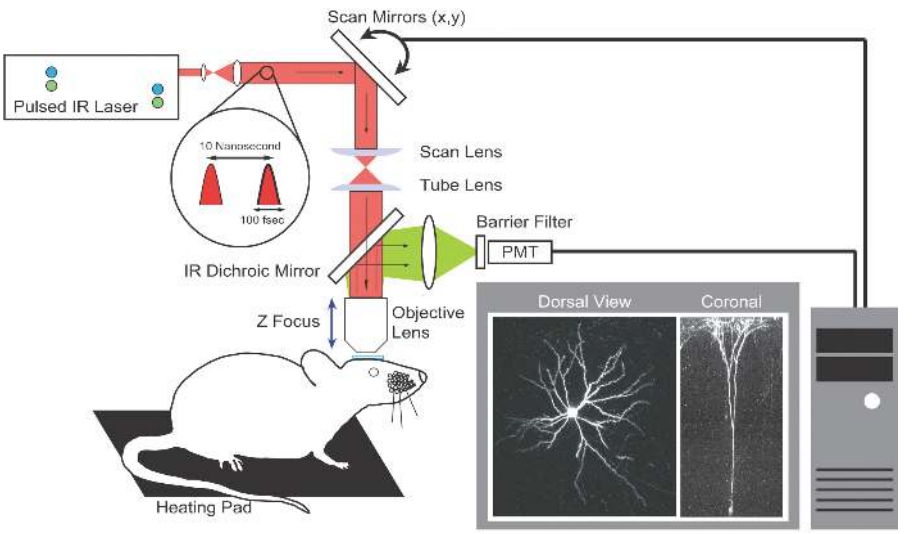

FIGURE 1. Two-photon laser-scanning microscopy in vivo. Images were acquired with a custom-built 2PLSM. The light source was a pulsed, mode-locked pulsed Titanium:Sapphire laser running at Λ ~910 nm. The repetition rate was ~100 MHz and the pulse duration ~100 fsec. The power measured at the back-focal plane of the objective was <200 mW. The laser beam is expanded and coupled into a pair of galvanometer scan mirrors. The mirrors are imaged onto the back-focal plane of the objective using a scan lens and a microscope tube-lens. The objective (typically Zeiss, 40X, 0.8 NA) focuses the excitation beam to a diffraction-limited spot. Fluorescence photons collected by the objective are reflected by a dichroic mirror and imaged onto a PMT detector. The image is constructed in a computer. (For color figure, see doi:10.1101/pdb.prot4902 online at www.cshprotocols.org.)

METHOD

Preparation of Mice for Imaging: Surgical Methods

1. Deeply anesthetize transgenic mice with an intraperitoneal injection of xylazine/ketamine for imaging (using 0.13 mg ketamine/g body weight and 0.01 mg xylazine/g body weight), or with an intraperitoneal injection of urethane (20%) (1.5 mg urethane/g body weight) for acute experiments. Monitor the depth of anesthesia periodically by lack of a toe-pinch reflex.
2. Administer dexamethasone (0.02 mL at 4 mg/mL) subcutaneously to minimize the cortical stress response during chronic experiments.
3. Sterilize all surgical tools and remove the flap of skin (~1 cm^2) covering the skull over the barrel cortex.
4. Remove all underlying fascia and push the lateral muscle (temporalis) ventrally, avoiding bleeding.
5. Apply a thin layer of cyanoacrylate to the skull and wound margins to stop bleeding and prevent the seepage of serosanguinous fluid.
   Optional: Apply a small amount of dental acrylic over the muscle and wound margins to seal the circumference.
6. Mark the cortical area of interest (barrel cortex at P35 is –2-mm Bregma, 4.25-mm lateral).
7. Use a dental drill (1/4 bit) to slowly thin the circumference of a 5 × 5-mm^2 region of the skull. Avoid overheating, which would cause bruising of the dura. Take care not to puncture the thinned skull while drilling.
   *The cortical surface vasculature should be visible where the skull is thinned and there should be minimal bleeding from the skull and none from the brain (*Fig. 2A*).*
8. Use a sharp syringe to gently and superficially perforate the thinned skull. Lift up the skull, exposing the dura. Use Gelfoam (cut into ~7-mm^2 blocks and presoaked in sterile cortex buffer) to control any bleeding from the dura and skull.
9. Construct an optical chamber by covering the clear, unblemished dura with a thin layer of agarose (1.5%) for neocortex imaging and a custom-made circular coverglass (7-mm diameter, No. 1 thickness), flush with the skull. Remove the extraneous agar and dry the remaining liquids on the skull (Fig. 2B).
10. Seal the optical window with dental acrylic, covering the exposed skull, wound margins, and coverglass edges. Embed a clean, small, titanium bar with tapped screw holes into the acrylic to stabilize the animal for subsequent imaging sessions, keeping the screw threads clear of acrylic (Fig. 2C). Allow the acrylic to dry thoroughly before manipulating the mouse or the frame.

Imaging

If acute experiments are to be performed, proceed to Step 11. For chronic experiments, proceed to Step 12.

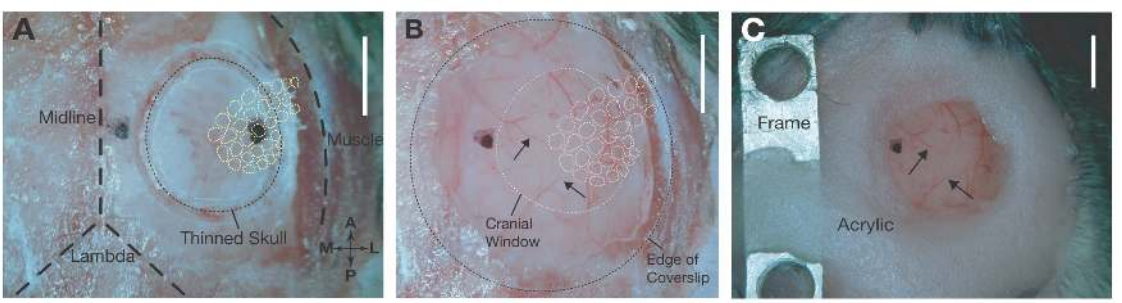

FIGURE 2. Experimental preparation for in vivo imaging. (*A*) The circumference of the region of skull to be excised is thinned. Black pen marks are used to align barrel cortex. The diameter of the craniotomy is ~4 mm. (*B*) The intact, exposed dura is covered with agar and a circular coverglass. (*C*) A small frame is embedded in dental cement to stabilize imaging. Arrows point to surface blood vessels. Bars, 2 mm. (For color figure, see doi:10.1101/pdb.prot4902 online at www.cshprotocols.org.)

11. Perform acute experiments for the duration of the anesthesia (typically up to 1 h after surgery for xylazine/ketamine or for 5 h under urethane anesthesia). Proceed to Step 13.

12. For chronic experiments, return the mouse to its cage after surgery and allow 7-10 d for recovery before imaging. For chronic imaging of ~45 min daily, use a dose of anesthesia that is one-half the surgical dose, or 0.075 mg/g ketamine and 0.005 mg/g xylazine. To reduce stress for the mouse, minimize the size of the metal frame used to stabilize the head so that the mouse can freely move in its cage.

    The cranial window can remain clear for months, without the use of antibiotics.

13. Proceed with imaging experiments.

TROUBLESHOOTING

Problem: The resolution for chronic imaging is not sufficiently high.

[Step 13]

Solution: If the transgenic mouse line chosen for in vivo imaging expresses the fluorescent protein at high enough concentrations in the cells of interest, the limiting steps to high-resolution chronic imaging are in the protocol itself. Optimize performance of the protocol steps as follows:

- Perform sterile surgeries consistently and quickly, and make sure that the mouse's head and body are stabilized.
- Make sure that the imaging window is optically clear throughout the long-term imaging period, aside from eventual regrowth of the skull after a few months. Keep the surgeries as sterile as possible, and avoid bleeding from the dura. During the surgery, absorb the blood with moist Gelfoam, allowing it to clot after a few minutes.
- Take care not to damage the dura by overheating during excessive skull thinning: Keep the skull moist and cool during drilling.
- In the properly stabilized anesthetized mouse, movement artifacts should not occur during imaging if the precise amount of agarose is applied. This can be achieved with practice by varying the viscosity, concentration, and amount of agar applied after skull removal. As long as the regions of interest remain unobscured, high-resolution in vivo imaging of the fine structure of neurons can be performed daily for time scales of months.

DISCUSSION

Our first attempts at imaging dendritic structures over time scales of days were in the developing rat barrel cortex, using Sindbis-virus-mediated expression of enhanced GFP in neurons (Chen et al. 2000). This approach has fundamental limitations. First, Sindbis virus is cytotoxic after ~4 d of expression, principally due to high levels of foreign gene expression (Agapov et al. 1998). Second, the rat dura mater degrades image quality. Nevertheless, the same neuron and dendrites could be imaged for a few days. These disadvantages were overcome by the development of transgenic mice that express spectral variants of GFP at high levels in cortical pyramidal neurons (Feng et al. 2000). We have used two lines with different expression patterns (YFP-H and GFP-M) (Fig. 3). In both lines, XFP expression is sufficiently high to image individual dendritic spines in vivo. In the GFP-M mouse, neurons are labeled in a sparse manner, but the labeled cells express GFP at high concentrations, giving the appearance of Golgi stains. In addition, the mouse dura is sufficiently thin so that it can be left intact without degradation of imaging. In these mice, neuronal structure was imaged chronically through an optical chamber (Levasseur et al. 1975; Brown et al. 2001; Trachtenberg et al. 2002). These optical chambers are hermetically sealed and maintain the cortical environment intact with respect to, for example, intracranial pressure, cerebral fluid composition, and prevailing gas tensions (Fig. 2).

The health of the cortex under the cranial window was verified electrophysiologically, anatomically, and ultrastructurally. Whisker stimulation evoked normal local field potentials and intracellularly recorded post-synaptic potentials in neurons in the barrel cortex underlying the optical window even after the optical window had been left in place for a number of weeks. Additionally, membrane potential measurements from cells immediately below the imaging window were not significantly different from those recorded from neurons in normal age-matched controls. Cortical circuitry was similarly

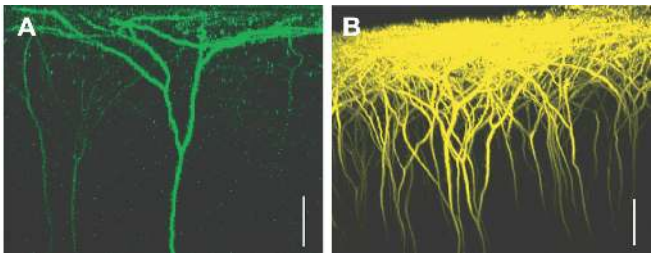

FIGURE 3. In vivo images of the upper layers of cortex in transgenic mice expressing YFP and GFP. Both mouse lines express fluorescence mostly in Layer V pyramidal neurons in the cortex. (*A*) Coronal view in a GFP-M mouse. (*B*) Coronal view in a YFP-H mouse. The dense expression pattern, compared to the GFP-M line, obscures individual Layer I dendrites. Side views are maximal projections in the *x* or *y* dimension (with *z* distance along the ordinate axis). Bars, 50 µm. (For color figure, see doi:10.1101/pdb.prot4902 online at www.cshprotocols.org.)

unaffected by the imaging window. Spontaneous synaptic activity and spontaneous fluctuations of membrane potentials, which reflect the strengths of synaptic inputs, were identical in implanted animals and controls (Trachtenberg et al. 2002). Anatomically, densities of spines measured in fixed brains were not different from densities immediately below the imaging window. In addition, the spine density in our in vivo images (0.392 ± 0.01 spines/µm) did not vary with experimental duration and is identical to measurements in fixed tissue from the same animals. Nor was there any indication of tissue damage at the ultrastructural level. Hallmarks of cortical damage, such as reactive microglia and increased extracellular space, were not observed in tissue that had been chronically imaged in vivo and subsequently examined under an electron microscope (Trachtenberg et al. 2002).

In each animal, the dendrites of a single Layer II/III or V pyramidal neuron and their spines can be imaged daily for several weeks. The cell and the respective regions of interest can be located each day by using the unique vascular pattern in the cortex as a reference. By using a picture of the surface vasculature taken on the first day of imaging with a digital camera (Fig. 2), the blood vessels can be aligned each day and the objective can be positioned within a distance of ~100 µm of the cell. The unique branching patterns of the fluorescent dendrites are then used to identify those specific regions of the cell that were imaged previously (Fig. 4). Fortunately, dendrites do not grow or retract appreciably in the adult cortex (Trachtenberg et al. 2002) and are easily identifiable each day. In the example in Figure 4, all dendrites that were imaged on the first day are reidentified in subsequent imaging sessions. For each cell, typically up to 10 fields of view of 45 × 45 µm can be selected for imaging. At this magnification, dendritic spines are clearly resolvable, and images are acquired at 512 × 512 pixels, or ~0.0879 µm/pixel, with 1-µm *z*-steps (Fig. 5). With the use of 2PLSM, it is straightforward to simultaneously excite two fluorophores with the same excitation wavelength. The emitted fluorescence can be separated spectrally using a dichroic mirror and detected using a pair of photo detectors. For example, we have injected Alexa Red-Dextran into the tail vein of a transgenic mouse and

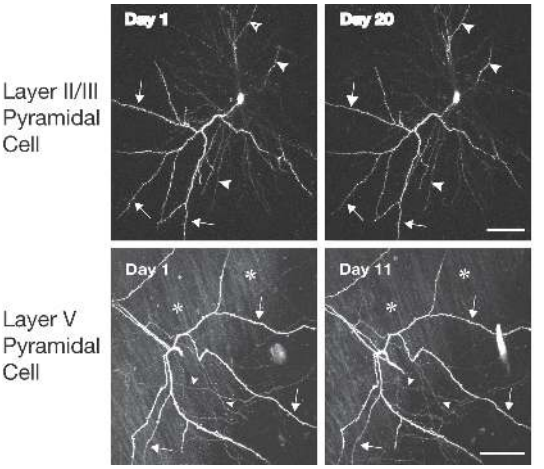

FIGURE 4. Long-term chronic imaging of GFP-expressing pyramidal neurons in adult mice. Typical examples of dendrites imaged over long times in vivo, shown as a projection of a stack of optical sections. (*Top*) Layer II/III pyramidal neuron was imaged over its full extent for 20 days. Both apical (arrows) and basal (arrowheads) dendrites are shown. Note that the basal dendrites appear dim due to their deep (~300 µm) location. (*Bottom*) Apical dendritic tufts of a Layer V pyramid extending into Layer I. Both dendritic branches (arrows) and axons (arrowheads) were stable. Vertical streaks (asterisks) are caused by autofluorescence in the dura, in the most superficial optical sections. Bars, 50 µm.

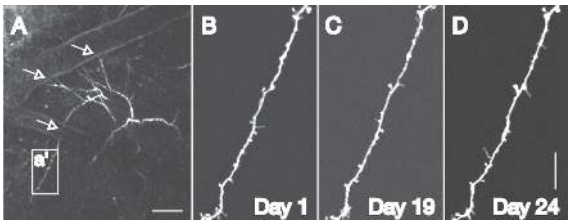

FIGURE 5. Long-term chronic in vivo imaging of dendritic spines. (*A*) Low magnification of a Layer V neuron apical dendritic tuft, shown as an *x-y* projection. Arrows point to locations where dendrites were hidden by surface blood vessels. Bar, 50 µm. (*Inset*) Region *a'* was imaged over a period of 25 days. Examples of the images of this region taken at days 1, 19, and 24 are given in *B*, *C*, and *D*, respectively. Bar, 10 µm.

imaged the neocortical vasculature with respect to fluorescent neurons (Fig. 6). The imaging of tiny structures, such as dendritic spines, has certain limitations. The axial resolution of our three-dimensional images is limited to >1.5 µm (Pawley 1995). We therefore cannot reliably resolve spines that project mainly along the optical axis, below or above the dendrite. In addition, because imaging conditions can change over the long experimental time scales, we adjust the excitation intensity with each imaging session to keep the brightness of the parent dendrite constant, thus achieving similar fluorescence levels for every time point. The excitation intensity for imaging spines should be sufficiently high to detect all, including the dimmest, spines.

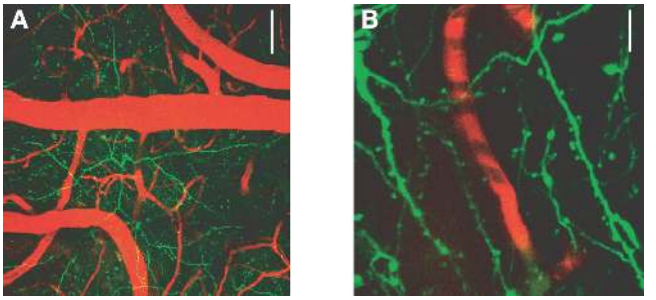

FIGURE 6. Dual-color in vivo imaging of blood flow and neurons in an adult mouse. A red dye (Alexa Red-Dextran) was injected into the tail vein of a GFP transgenic mouse, labeling the vasculature in the brain (red). (*A*) Top view of apical dendrites expressing GFP (green) and cortical blood vessels filled with Alexa Red-Dextran (red). Bar, 50 µm. (*B*) Higher-magnification view of axons and dendrites intermingled with capillaries. The dark stripes in the blood vessels indicate the excluded volumes of the nonfluorescent red blood cells. Bar, 10 µm. (For color figure, see doi:10.1101/pdb.prot4902 online at www.cshprotocols.org.)

To identify the position of an imaged cell, for example, in relation to the barrel cortex map, red fluorescent latex microspheres are pressure-injected into the cortex using a glass micropipette at the end of the final imaging experiment. Several injections are made as close to the cell of interest as possible using the digital pictures of the unique vascular profile around the cell to position the micropipette tip. Mice are then transcardially perfused with 4% paraformaldehyde in 0.1 M sodium phosphate buffer. The hemisphere containing the imaged cell is removed, flattened, and post-fixed for 24-48 h. Vibratome sections (100 µm) are then cut tangential to the cortical surface, and the sections containing the Layer IV barrels (usually sections 2-5) are stained for cytochrome oxidase. The first section, which usually contains the imaged apical dendrites, is used to determine the position of the injected beads relative to the position of the cell. Once this is known, the position of the cell relative to the barrel map is then determined by finding the position of the red fluorescent beads in the cytochrome-oxidase-stained sections containing the barrel map.

REFERENCES

Agapov, E.V., Frolov, I., Lindenbach, B.D., Pragai, B.M., Schlesinger, S., and Rice, C.M. 1998. Noncytopathic Sindbis virus RNA vectors for heterologous gene expression. *Proc. Natl. Acad. Sci.* **95:** 12989–12994.

Brown, E.B., Campbell, R.B., Tsuzuki, Y., Xu, L., Carmeliet, P., Fukumura, D., and Jain, R.K. 2001. In vivo measurement of gene expression, angiogenesis and physiological function in tumors using multiphoton laser scanning microscopy. *Nat. Med.* **7:** 864–868.

Chen, B.E., Lendvai, B., Nimchinsky, E.A., Burbach, B., Fox, K., and Svoboda, K. 2000. Imaging high-resolution structure of GFP-expressing neurons in neocortex in vivo. *Learn. Mem.* **7:** 433–441.

Denk, W., Strickler, J.H., and Webb, W.W. 1990. Two-photon laser scanning microscopy. *Science* **248:** 73–76.

Feng, G., Mellor, R.H., Bernstein, M., Keller-Peck, C., Nguyen, Q.T., Wallace, M., Nerbonne, J.M., Lichtman, J.W., and Sanes, J.R. 2000. Imaging neuronal subsets in transgenic mice expressing multiple spectral variants of GFP. *Neuron* **28:** 41–51.

Kleinfeld, D., Mitra, P.P., Helmchen, F., and Denk, W. 1998. Fluctuations and stimulus-induced changes in blood flow observed in individual capillaries in layers 2 through 4 of rat neocortex. *Proc. Natl. Acad. Sci.* **95:** 15741–15746.

Levasseur, J.E., Wei, E.P., Raper, A.J., Kontos, A.A., and Patterson, J.L. 1975. Detailed description of a cranial window technique for acute and chronic experiments. *Stroke* **6:** 308–317.

Oheim, M., Beaurepaire, E., Chaigneau, E., Mertz, J., and Charpak, S. 2001. Two-photon microscopy in brain tissue: Parameters influencing the imaging depth. *J. Neurosci. Methods.* **111:** 29–37.

Pawley, J.B. 1995. *Handbook of biological confocal microscopy*. Plenum Press, New York.

Trachtenberg, J.T., Chen, B.E., Knott, G.W., Feng, G., Sanes, J.R., Welker, E., and Svoboda, K. 2002. Long-term in vivo imaging of experience-dependent synaptic plasticity in adult cortex. *Nature* **420:** 788–794.

Long-Term, High-Resolution Imaging in the Neocortex In Vivo

Brian E. Chen, Joshua T. Trachtenberg, Anthony J.G.D. Holtmaat and Karel Svoboda

Cold Spring Harb Protoc; doi: 10.1101/pdb.prot4902